

# PCCP

Accepted Manuscript



This is an *Accepted Manuscript*, which has been through the Royal Society of Chemistry peer review process and has been accepted for publication.

*Accepted Manuscripts* are published online shortly after acceptance, before technical editing, formatting and proof reading. Using this free service, authors can make their results available to the community, in citable form, before we publish the edited article. We will replace this *Accepted Manuscript* with the edited and formatted *Advance Article* as soon as it is available.

You can find more information about *Accepted Manuscripts* in the [Information for Authors](#).

Please note that technical editing may introduce minor changes to the text and/or graphics, which may alter content. The journal's standard [Terms & Conditions](#) and the [Ethical guidelines](#) still apply. In no event shall the Royal Society of Chemistry be held responsible for any errors or omissions in this *Accepted Manuscript* or any consequences arising from the use of any information it contains.

Cite this: DOI: 10.1039/c0xx00000x

www.rsc.org/xxxxxx

ARTICLE TYPE

# Beyond the Volcano Limitations in Electrocatalysis - Oxygen Evolution Reaction

Niels Bendtsen Halck<sup>a</sup>, Valery Petrykin<sup>b</sup>, Petr Krtil<sup>\*b</sup> and Jan Rossmeisl<sup>\*a</sup>

Received (in XXX, XXX) Xth XXXXXXXXXX 20XX, Accepted Xth XXXXXXXXXX 20XX

DOI: 10.1039/b000000x

Oxygen evolution catalysis is restricted by the interdependence of adsorption energies of the reaction intermediates on the surface reactivity. The interdependence reduces the number of degrees of freedom available for catalyst optimization. Here it is demonstrated that this limitation can be removed by active site modification. This can be achieved on ruthenium by Ni or Co incorporation into the surface, which activates a proton donor /acceptor functionality on the conventionally inactive *bridge* surface sites. This enhances the actual measured oxygen evolution activity of the catalyst significantly compared to conventional ruthenium.

## Introduction

Electrocatalytic energy conversion and storage have gained in importance recently mainly in connection with the growing role of renewable energy sources<sup>1</sup>. Fundamentally, the underlying electrocatalytic reactions are redox processes of multi-electron nature and can be perceived as a sequence of single electron charge transfer steps. These processes are also – as a rule – kinetically hindered and require a substantial energetic driving force to proceed at technologically acceptable rates.

Regardless of the nature of the electrocatalytic process, it has to follow through surface confined reaction intermediates. This means that the driving force can be minimized and the catalysts activity thereby optimized if the binding of the reaction intermediates is matched. The ideal catalyst is showing appreciable activity at virtually zero driving force. Such an “ideal electrocatalyst” needs to have equidistant distribution of the free energy in each individual charge transfer step of the whole reaction sequence. Rational catalyst design, therefore, can be viewed as an attempt to fine tune the energetics of the charge transfer reactions to achieve the equal distribution of the free energy in all steps of the reaction sequence<sup>2</sup>. This is equivalent to optimization of the relative strength of the intermediate(s) bonding on the catalysts surface, which can be theoretically assessed using density functional theory (DFT)<sup>3</sup>. The DFT consequently can be used to estimate the driving forces needed in each individual charge transfer step. This represents the thermodynamic limit of the overall reaction kinetics. The catalyst design is, therefore, reduced to finding a material featuring optimal binding of all intermediates and consequently an optimal activity.

The real catalyst's design is, however, hindered by the interdependence of two or more reaction steps. The binding of the intermediates tends to show the same linear scaling with the catalyst's reactivity, which reduces the number of degrees of freedom (tunable parameters) available for the catalyst's optimization. The reactivity which is the only tuneable parameter

can therefore be used as activity descriptor. Due to only one available tuneable parameter one can doubt the possibility to design catalysts approaching the thermodynamic limit.

This conceptual restriction, often described as the universality of the scaling relations, has been verified for various electrocatalytic processes including oxygen evolution<sup>4</sup>, oxygen reduction<sup>5</sup>, and methanol oxidation<sup>6</sup> as well as for various classes of electrocatalytic materials including metals<sup>7</sup>, oxides (sulfides, nitrides)<sup>8</sup>, or molecular catalysts<sup>9</sup>. Therefore it seems to be an inherent limit of the rational design of electrocatalysts for the multiple electron redox process. Breaking the scaling relationship(s) allowing for independent binding energy optimization of the reaction intermediates represents in this respect a major challenge for both theoretical and synthetic chemistry. It represents also the only way for qualitative improvement of the catalytic performance beyond the state of the art. The most intuitive approach to break the scaling relationships is to modify the active site by changing from a surface catalyst to a three dimensional active site<sup>4</sup>. However, so far none of the suggestions has been successfully realized.

The oxygen evolution reaction (OER) serves as a suitable model system. It combines sufficient simplicity with practical importance as OER represents the limiting process in the generation of hydrogen in electrochemical or photo-electrochemical water splitting<sup>10</sup>.

The oxygen evolution process is a four electron oxidation process driven by a transfer of 4.92 eV per oxygen molecule, i.e., 1.23 eV per electron. Experiments identify the second or third electron transfer as the rate limiting step regardless of the nature of the electrode material<sup>11</sup>. The theoretical analysis of the problem concurs with the experimental assessment. The free energy required for the second charge transfer step is identified as an universal single descriptor of the oxygen evolution process<sup>4</sup>. The definition of the descriptor reflects the fact that the intermediates yielded in the first and third charge transfer step show the same scaling with the surface reactivity.

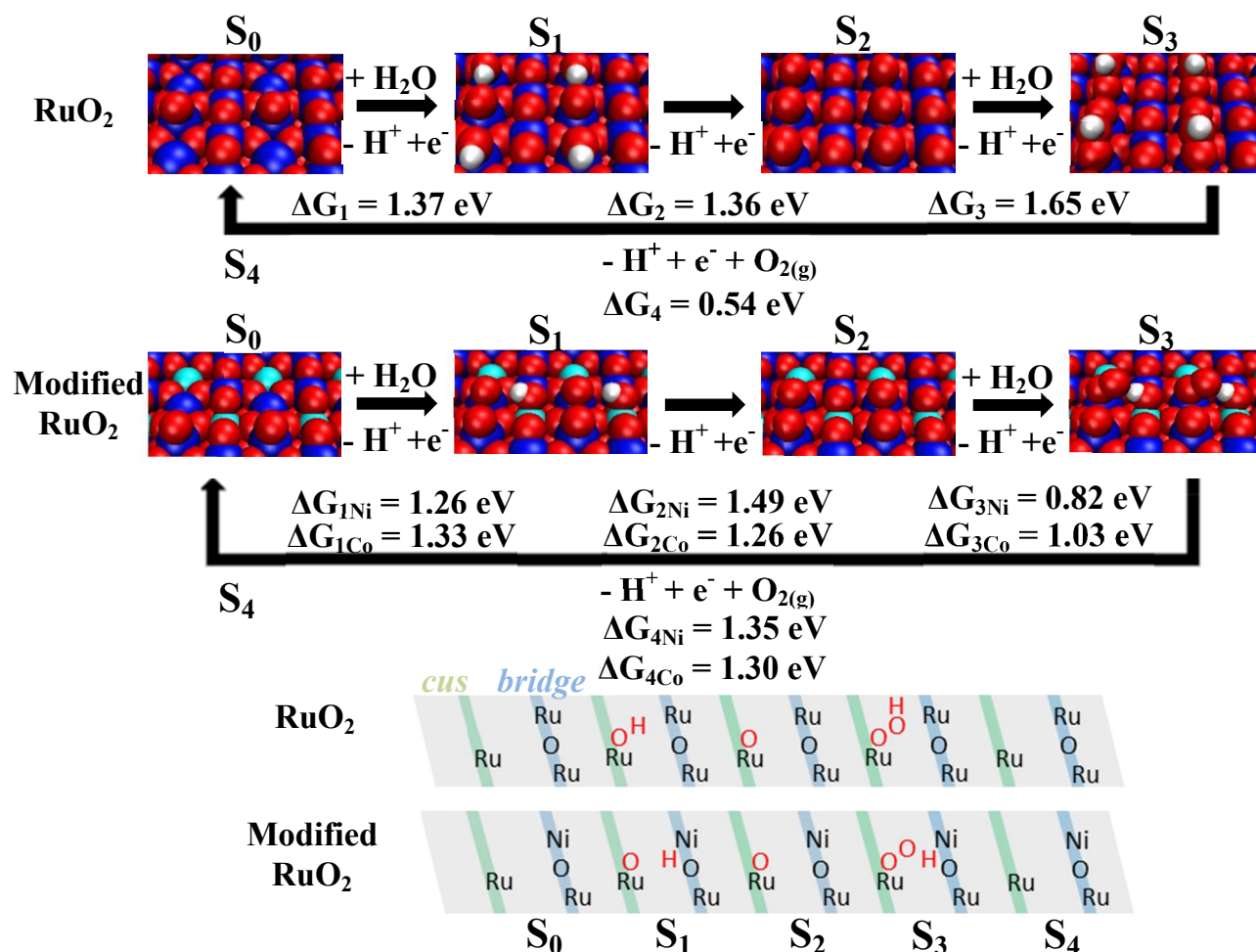


**Figure 2:** Reaction mechanism of the oxygen evolution reaction on conventional rutile ruthenia and Ni and Co modified ruthenia on the {110} surface. The Gibbs free energies obtained from DFT calculations are for each of the reaction steps is included. For Ni and Co modified ruthenia the first and third step deviates in energy due to the activating bridging O atom which binds the proton. Color coding of the atoms: O – red, Ru – blue, Ni or Co – Cyan, H – white. Below is a schematic figure of the role of the two binding sites for ruthenia and Ni modified ruthenia. The green row represents the *cus* row and the blue row represents the *bridge* row and red highlight intermediates.

Regardless of the catalyst, the free energies of the \*OH and \*OOH intermediates show a constant difference of approximately 3.2 eV<sup>4,12</sup>. This constant difference is ca. 0.8 eV higher than the desired 2.46 eV of an ideal catalyst with equidistant free energy steps. This defines the smallest theoretically conceivable overpotential needed to drive the oxygen evolution to approximately 0.4 V. Although the theoretical description in principle allows for catalyst design and optimization, the 0.4 V penalty represents a limitation applicable to all the catalysts so far considered<sup>4,13,14</sup>. It needs to be stressed, that the studies reporting so far on the rational design (i.e. a combination of the theoretical prediction with targeted synthesis) to optimize the electrocatalytic activity in oxygen evolution remain within this paradigm and utilize combinatorial screening to optimize a single descriptor of the surface reactivity. Resulting materials - although offering a variability of the catalysts' electronic structure - cannot break the limitation put forward by the scaling relations described above and summarized in the volcano curves.

Restricting the considerations to rutile type oxide catalysts, which represent industrial benchmark materials for OER, one may confine the actual activity to so called coordination unsaturated sites (*cus*) present on the surface<sup>15</sup>. The *cus* sites can be identified

with surface metal cations which form (n-1) bonds with oxygen (where n is the number of oxygen bonds formed by the given cation in the bulk). Only *cus* sites allow for formation of reactive "atop" positions essential for formation of strongly adsorbed intermediates<sup>15</sup>. Of the rutile oxides ruthenia (RuO<sub>2</sub>) is known to be particularly active in the oxygen evolution as confirms also the theoretical analysis which places this oxide close to the top of the volcano. It was reported that even in the case of ruthenia based catalysts the activity gets improved by a controlled incorporation of the hetero-valent cations<sup>16</sup>. It may be envisaged that the *cus* site architecture may be artificially modified by the heterovalent cation incorporation. This communication elaborates possible effects of the local structure modifications on the resulting oxygen evolution activity and presents a general approach capable of breaking the universal scaling relationships of the OER. The general nature of this approach is demonstrated by a DFT based theoretical analysis of the OER activity of modified ruthenia catalysts combined with their experimental behaviour.

## Methods

Ni and Co incorporated nanocrystalline ruthenia catalysts were prepared by co-precipitation of alcohol based solution ruthenium(III) nitrosyl nitrate with stoichiometric amount of  $\text{Ni}(\text{NO}_3)_2$  or  $\text{Co}(\text{NO}_3)_2$  by tetramethylammonium hydroxide. Precipitate was aged in a PTFE lined autoclave at  $120^\circ\text{C}$  for 24 hours. The resulting precursor was filtered, dried and annealed at  $400^\circ$  for 3 hours to obtain crystalline catalysts. Details of the synthesis and characterization can be found in<sup>17,18</sup>. The reference samples of  $\text{IrO}_2$  and  $\text{MnO}_2$  were prepared by hydrothermal synthesis from iridium(III) acetylacetonate (Alfa Aesar) and potassium permanganate (Aldrich), respectively. The electrodes for electrochemical experiments were prepared from synthesized materials by sedimentation of nanocrystalline powder from a water based suspension (5 g/L) on Ti mesh (open area 20%, Goodfellow) to obtain the surface coverage of about 1-2  $\text{mg}/\text{cm}^2$  of active oxide. The deposited layers were stabilized by annealing the electrodes for 20 min at  $400^\circ\text{C}$  in air. The electrocatalytic activity of the prepared materials with respect to oxygen evolution was studied in potentiostatic experiments in a 0.1 M  $\text{HClO}_4$  solution. All experiments were performed in a homemade Kel-F single compartment three electrode cell controlled by a PAR 263A potentiostat. Pt and saturated calomel electrode (SCE) were used as an auxiliary and a reference electrode, respectively. All potentials shown in the text were recalculated and are quoted with respect to RHE.

The model structures used in DFT calculations were based on local structure as obtained in a refinement of EXAFS functions processed from the X-ray absorption spectra (XAS) measured on Ru, Ni and Co K absorption edges. Details of these experiments are given in Supplementary information.

The DFT binding energies are calculated using software where the valence electronic states are described by a plane wave basis and the core-electron interactions with Vanderbilt ultrasoft pseudopotentials<sup>19</sup>. For all surfaces the exchange-correlation functional Revised Perdew-Burke-Ernzerhof (RPBE) was used<sup>20</sup>. The planewave basis used a cutoff of 350 eV for the kinetic energy and a 500 eV cutoff for the density. A  $4 \times 4 \times 1$  Monkhorst-Pack grid was used to sample the Brillouin zone of the system. The conventional rutile ruthenia {110} surface is modelled using a  $1 \times 2$  supercell with 4 atomic trilayers as described in literature<sup>4</sup>. The Ni modified {110} surface is modelled using a larger  $1 \times 3$  supercell with 1 Ni in the *bridge* row and 1 Ni in the *cus* row as shown on Figure 1 together with other possible local arrangements. The calculations are spinpolarized.

## Results and Discussion

The  $\text{Ni}^{17}$  and  $\text{Co}^{18}$  incorporated ruthenia conform apparently to a single phase rutile structure featuring an uneven distribution of the structure incorporated cation. EXAFS based structural studies prove that the Ni and Co cations show a strong tendency to form clusters coordinated along (111) direction of the rutile structure rather than distribute homogeneously in the ruthenium rich oxide framework. Despite the apparently intact translational order of the Ni and Co modified oxides, the cation introduction alters the local structure of the catalyst in the way shown in Figure 1S. Regardless of the nature of the structure incorporated cation, the mechanism compensating for lower charge of the Ni and Co cations suppresses the clustering of cations along the (001) direction. Assuming a surface structure conforming to this constraint one can construct three principal arrangements shown in Figure 1. These may feature isolated heteroatoms in either *cus* or *bridge* position (Figure 1a) separated by cationic sites occupied by Ru atoms. Alternatively one may assume a presence of short chains of the heteroatoms (2-3)

stacking along (001) direction either in *bridge* or *cus* position forming an isolated island in the surface (Figure 1b and c).<sup>17</sup>

The functionality of these principal arrangements is visualized in the DFT calculations assuming smallest unit cell featuring all needed local arrangements (see Figure 1a). The overall energetics of the oxygen evolution process on the Ni modified ruthenia (see Figure 2) and shows significant deviation from that of conventional ruthenia. The potential step that requires the highest potential has changed from the third electron removal for conventional ruthenia to the second electron removal for the Ni modified ruthenia and the first electron removal for the Co modified ruthenia. The biggest free energy step amounts to 1.49 eV and 1.33 eV for the Ni and Co modified ruthenia, respectively, (see Figure 2) as compared to 1.65 eV for conventional ruthenia. This allows us to estimate the thermodynamic limit of the overpotential of the whole process to  $\sim 0.3\text{V}$  for Ni modified ruthenia and  $\sim 0.1\text{V}$  for Co modified ruthenia. These overpotentials are significantly lower than the minimum overpotential of 0.4V predicted previously<sup>4</sup> which is mainly due to lowering of the energy of the  $\text{S}_3$  state compared to conventional ruthenia as seen on Figure 3. The increase in activity compared to conventional ruthenia are met in the experiments (see Figure 4) to some degree where cation modified ruthenia shows a greater activity compared with conventional ruthenia.

The results of the DFT modelling rationalize the effect of the introduction of Ni or Co on the ruthenia surface. The presence of Ni or Co at the *cus* positions has only negligible effect on the binding properties of the predominantly Ru composed surface. The binding energy of oxygen on the catalytically active Ru *cus* site is 2.75 and 2.59 eV for Ni and Co in the bridge site respectively while for conventional ruthenia the binding of O in the same position is 2.73 eV (see Table 1S and Figure 3). In this way the presence of Ni or Co in *cus* site cannot be related to the observed increase in the oxygen evolution activity of the Ni or Co modified ruthenia. The available *bridge* positions generally deemed non-participating in the oxygen evolution process get activated by the presence of Ni or Co, which allows for simultaneous electron/proton transfer at the potential close to the standard potential of the oxygen evolution process. The activation of the *bridge* site as a proton donor/acceptor effectively introduces a second tuneable parameter of the oxygen evolution process as the bridging O adsorbs hydrogen from the  $\text{*OH}$  in  $\text{S}_1$  and  $\text{*OOH}$  species in  $\text{S}_3$  (Figure 2) which lowers the energies of

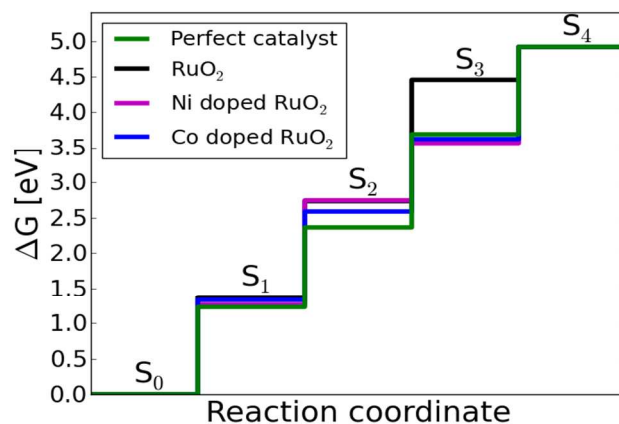


**Figure 3:** Free energy diagram based on DFT calculations for conventional, Ni and Co modified ruthenia and the perfect catalyst for the four steps in the oxygen evolution reaction mechanism. The modified ruthenia catalysts has a significant stronger binding in  $\text{S}_3$  which is the potential limiting step for ruthenia.



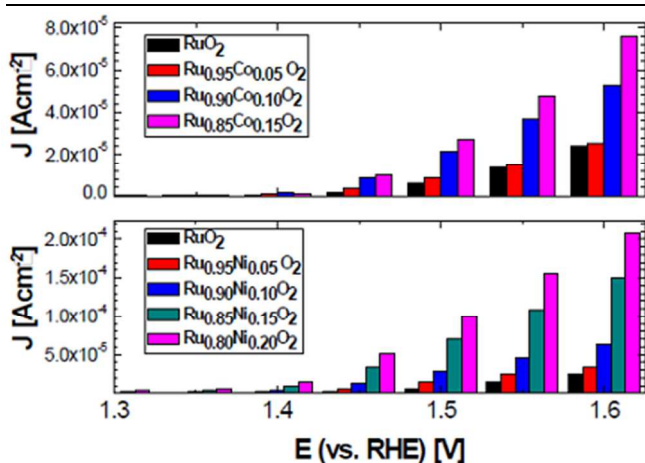


**Figure 4:** The current density of oxygen evolution on Ni and Co modified ruthenia in 0,1M HClO<sub>4</sub>. The data were extracted from potentiostatic experiments 40s after potential application.

these states compared to conventional ruthenia. The reactivity of the surface *cus* sites and the *bridge* site proton donor/acceptor potential are still weakly correlated via a hydrogen bond, which affects the oxidation potential of the *bridge* site if oxygen is present on the adjacent *cus* site. For Ni and Co modified ruthenia the potential for removing the proton from the bridging oxygen with oxygen present of the ruthenium *cus* site is 1.33V-1.49V respectively and without oxygen on the *cus* site the potential for removing the proton is 1.23-1.33V respectively (see Table 1S in supplementary materials). An improvement of the oxygen evolution related catalytic activity in hematite with Ni and Co doping has also been reported but the observed effect is rather moderate which is likely due to a semiconducting nature of hematite.<sup>22</sup>

The DFT calculations show that the Ni and Co modified ruthenia still should lag behind the performance of an ideal catalyst. It is essential to stress, however, that the activation of the *bridge* sites removes the problem of the same free energy scaling of different intermediates providing the necessary degree of freedom to approach a global optimum via a new reaction pathway. Note that an adjustment of the donor/acceptor levels of the introduced cation is prerequisite for the oxygen evolution enhancement. Figure 5 shows that the apex of the “volcano curve” based on the scaling relationships appears at 1.6 eV, i.e. at somewhat higher descriptor value than that of the ideal catalysts (1.23 eV). The theoretical activity predicted for Ni and Co modified ruthenia appears significantly above the apex of conventional “volcano curve”. These catalysts continue on the weak binding leg of the volcano which is the dashed line on Figure 5 despite being in the strong binding region.

This situation can be rationalized keeping in mind that the proton/acceptor functionality represents additional descriptor not reflected in Figure 5. Figure 5, therefore, represents a one-dimensional reduction of a two dimensional volcano surface. In this two-dimensional approach the predicted catalytic activities would form a surface of a pyramid where the base is described by the reactivity of the surface *cus* sites and the *bridge* site proton donor/acceptor potential forming the *x* and *y* axes. In practical terms the introduction of the second parameter as seen for the oxygen evolution on Ni modified ruthenia, essentially outlines the simplest multi-dimensional approach allowing us to improve the electrocatalyst’s behavior beyond the limitations of a single descriptor “volcano curve”.

Although the experimental results do reflect an increase of the oxygen evolution activity upon modifying ruthenia with Ni or Co

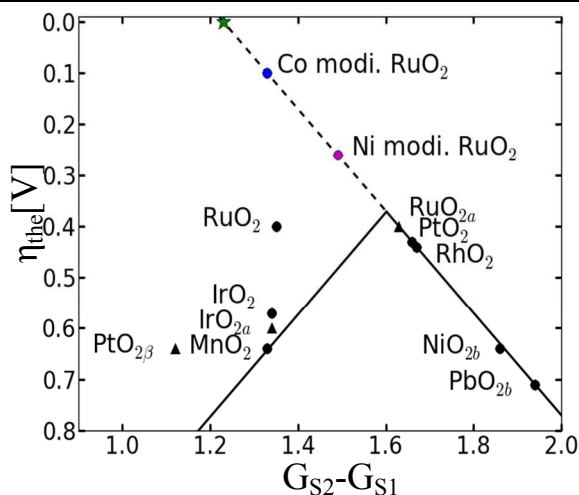


**Figure 5:** Volcano curve of the theoretical overpotential for oxygen evolution processes based on the DFT calculations described in literature<sup>4</sup> using the second charge transfer reaction as a descriptor. The star marks the position of an ideal catalyst, the magenta circle corresponds to Ni modified ruthenia and the blue circle to Co modified ruthenia.

the observed effect (see Figure 4) seem to be less significant than the theoretical predictions.

This discrepancy can be qualified realizing the conceptual difference between real catalyst and their model representation in the DFT calculations. While the DFT calculations are created by periodic replications of the modified active site (see Figure 1) the real catalysts feature only limited number of the modified active sites diluted in the ruthenia matrix. A correct correlation in such a case can be obtained if one uses the measured current density per active site which is corrected for the contribution of the regions containing no dopant.

These current densities can be calculated using a simple formalism anticipating that a presence of the each dopant atom in *bridge* or *cus* site is proportional to the total dopant concentration. In this case the site normalized current for cobalt modified ruthenia can be written as:

$$J(\text{RuMe}_{\text{site}}) = \frac{J(\text{RuMe}_x) - (1-x)J(\text{Ru})}{x} \quad (1)$$

where *x* stands for the Ni or Co fraction, *J*(RuMe<sub>*x*</sub>) and *J*(Ru) represent experimentally measured current density for modified

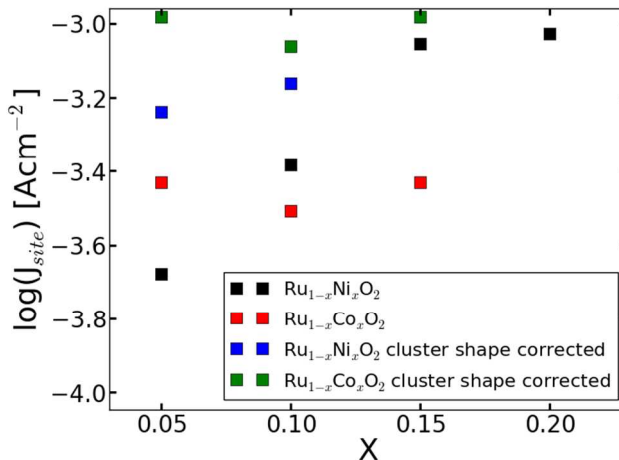


**Figure 6:** Site normalized oxygen evolution activity of Ni and Co modified ruthenia Ru<sub>1-x</sub>Ni<sub>x</sub>O<sub>2</sub> as a function of the Ni and Co content with (blue and green squares) and without cluster shape correction (red and black squares). Log denoted the base 10 logarithm.

and conventional ruthenia, respectively and  $J(\text{RuMe}_{\text{site}})$  stands for the site normalized current density.

While the site normalized current densities of the Co modified catalysts calculated for different overall Co content according to equation (1) are independent of concentration the site normalized current densities of the Ni modified materials remain concentration dependent shown on Figure 6. This behavior is caused by the concentration dependence of the Ni local environment. In the particular case of modified ruthenia, the Co modification forms a cluster structure which is independent of concentration whereas the Ni modified ruthenia tend to form clusters protruding preferentially in the  $\{110\}$  surfaces with increasing Ni content.

This clustering tendency violates the assumption expressed in the equation (1) since the probability of the Ni entering the activated bridge position increases above the proportionality if the total Ni content  $x$  exceeds 0.05. The deviation from the proportionality may be corrected if the structure of the cluster is taken into account. EXAFS based cluster structures applicable to Co and Ni modified structures are shown in Figure 1S of the supplementary information. While the structure shown in Figure 1Sa applies to all Co modified ruthenia but only applies for the modified structures with low Ni content ( $x=0.05$ ). The structure shown in Figure 1Sb is valid for Ni modified ruthenia with higher Ni content ( $x=0.1$ ). The cluster size can be conservatively estimated to 3 and 5 Ni atoms, respectively. The orientation of the clusters with respect to the  $\{110\}$  surface of the nanoparticles sets a correction factor  $y$  complementing the equation (1), which reflects the fraction of the cluster atoms possibly residing in  $\{110\}$  oriented surface.

$$J(\text{RuNi}_{\text{site}}) = \frac{J(\text{RuNi}_x) - (1-x)J(\text{Ru})}{xy} \quad (2)$$

This correction factor is equal to 1/3 and 3/5 for the structures shown in Figure 1Sa and b, respectively. The site normalized current densities reflecting the structure of the Co or Ni clusters are shown in Figure 6 (blue and green symbols). The correction for the size and structure suppresses the concentration dependence Ni clusters' site normalized activity. It needs to be noted that the site normalized activity of the Co modified materials remains higher than that of the Ni counterparts, although this difference decreases with increasing dopant's concentration. Superiority of the Co modified materials – particularly at low  $x$  generally agrees with the results of the DFT calculations.

DFT predicted thermodynamic limits to the overpotentials are often compared with the parameters used to describe the electrode kinetics – e.g. current density at chosen electrode potential. It has to be born in mind that DFT does not provide overpotential values that directly can be compared to experiments. Only the trends in results should be compared. This fact can be explored to compare the theoretically limiting overpotentials with the experimental current densities taken for different catalysts at the same electrode potential. Provided that electrode reaction on all compared electrode materials follows the same reaction mechanism one should reasonably assume the experimental current density to be an exponential function of the DFT predicted limiting overpotential which is shown on Figure 7 where the dependence of the experimental current density at 1.6 V (vs. RHE) of several known oxide electrocatalysts on the limiting activation barrier is compared. The significant increase in the site normalized oxygen evolution activity, however, also suggests rather low stability of the catalyst namely in the acid

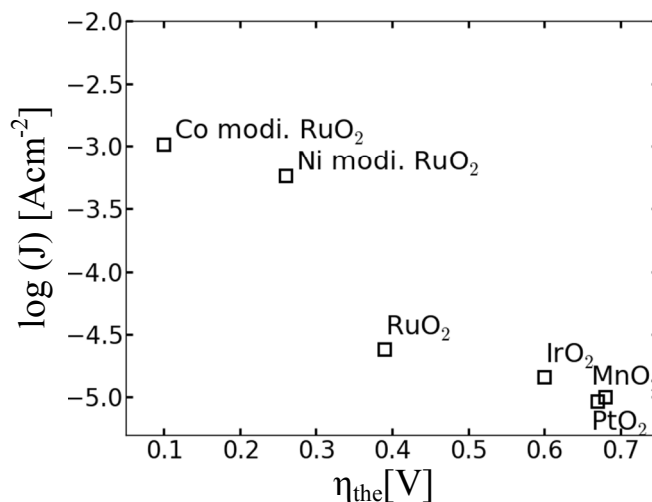


**Figure 7:** The correlation between the measured current density measured at 1.6V (vs. RHE) and the theoretical overpotential for different oxides. For the mixed oxides a concentration of Ni or Co of 0.05 is chosen to represent the activity per site for the cation modified ruthenia. More detailed information is available in the supplementary information.

media which is indeed confirmed by the spectroscopic measurements<sup>17</sup>.

Regardless of the low stability of the Ni or Co modified ruthenia – these catalysts are the first examples of circumventing the limitations set by the scaling relations. In this respect it needs to be accented that the observed phenomenon (introduction of proton acceptor/donor sites), although being intrinsic catalyst's property in this particular case, can in principle also be triggered by alternative mechanisms like, e.g. by anion<sup>23,24</sup> or CO<sup>25,26</sup> adsorption. This fact allows for a transfer of this approach to other electrocatalytic processes in aqueous media like, e.g. oxygen reduction<sup>27</sup> or CO<sup>28</sup> and CO<sub>2</sub> reduction<sup>29</sup>, if the electronic properties of the modified active site are fine-tuned with respect to the standard potential of the overall process. It also gives a clear indication that the rational design of the catalyst should aim at modification of the local structure of the catalytically active materials which is likely to result in metastable structures rather in stable ones which were in the center of exploration so far.

## 80 Conclusions

Theoretical analysis of the oxygen evolution on Ni and Co modified ruthenia catalysts shows, that the proton donor/acceptor functionality of the *bridge* site can be optimized independently of the surface reactivity at the *cus* sites, which results in significant reduction of the theoretical overpotential compared to the conventional ruthenia which is also reflected in the experimental work as Ni modified ruthenia is observed to be far more than active than conventional ruthenia beyond what the scaling relations predicts.

The addition of proton donor/acceptor functionality to the oxygen evolution reaction represents a simple multidimensional optimization of multi-electron electrocatalytic processes in aqueous media. This principle can be likely extended to other electrocatalytic processes and may represent a general concept of the rational catalyst design.

The comparison between experimental and theoretical work on modified ruthenia is complicated by the structural differences between Ni and Co clusters formed in the ruthenia matrix which why the per site normalization and the cluster correction is

needed to be applied before the experimental results can be compared to the per site activity obtained from DFT calculations.

## Acknowledgements

<sup>5</sup> The CASE initiative is funded by the Danish Ministry of Science, Technology and Innovation. Support from DCSC is gratefully acknowledged. V.P. and P.K. gratefully acknowledge the support of the Grant Agency of the Academy of Sciences of the Czech Republic under contract IAA400400906.

## Notes and references

<sup>a</sup> Center for Atomic-Scale Materials Design, Department of Physics, Technical University of Denmark, Building 307, 2800 Kgs. Lyngby, Denmark. E-mail: jross@fysik.dtu.dk.

<sup>b</sup> Department of Electrocatalysis, J. Heyrovský Institute of Physical Chemistry, Academy of Sciences of the Czech Republic, Dolejškova 3, 18223 Prague, Czech Republic. E-mail: Petr.Krtil@jh-inst.cas.cz

<sup>15</sup> † Electronic Supplementary Information (ESI) available: [Experimental procedure, active site model formulation, catalytic characterization and theoretical model of the oxygen evolution reaction]. See DOI: 10.1039/b000000x/

<sup>20</sup> ‡ Footnotes should appear here. These might include comments relevant to but not central to the matter under discussion, limited experimental and spectral data, and crystallographic data.

- <sup>25</sup> [1] Lewis N. S & Nocera D. G. *Proc. Natl. Acad. Sci. U.S.A.*, 2006, **103**, 15729.
- [2] Rossmeisl J. *et al.*, *J. Electroanal. Chem.*, 2007, **607**, 83.
- [3] Norskov J. K. *et al.*, *Nature Chem.*, 2009, **1**, 37.
- <sup>30</sup> [4] Man, I. C. *et al.*, *Chemcatchem*, 2011, **3**, 1159.
- [5] Stephens, I. E. L. *et al.*, *Energy & Environ. Sci.*, 2012, **5**, 6744.
- [6] Rossmeisl, J. *et al.*, *Energy & Environ. Sci.*, 2012, **5**, 8335.
- <sup>35</sup> [7] Abild-Petersen, F. *et al.*, *Phys. Rev. Lett.*, 2007, **99**, 016105.
- [8] Fernandez, E., *et al.*, *Angew., Chem., Int. Ed.*, 2008, **47**, 4683.
- [9] Calle-Vallejo, F., *et al.*, *Phys., Chem., Chem., Phys.*, 2011, **13**, 15639.
- <sup>40</sup> [10] Whitesides, G. M. & Crabtree, G. W., *Science*, 2007, **315**, 796.
- [11] Trasatti, S., *Electrochim. Acta*, 2000, **45**, 2377.
- [12] Koper M. T. M., *J. Electroanal. Chem.*, 2011, **660**, 254.
- <sup>45</sup> [13] Suntivich, J., *et al.*, *Science*, 2011, **334**, 1383.
- [14] Kanan, M.W. & Nocera, D.G., *Science*, 2008, **321**, 1072.
- [15] Hansen, H. A. *et al.*, *Phys. Chem. Chem. Phys.*, 2010 **12**, 283.
- <sup>50</sup> [16] Petrykin, V., Macounova, K., Shlyakhtin, O. A. & P. Krtil., *Angew. Chem. Int. Ed.*, 2010, **49**, 4813.
- [17] Petrykin, V. *et al.*, *J. Phys. Chem. C*, 2009, **113**, 21657.
- [18] Petrykin, V., *et al.*, *Catal. Today*, 2013, **202**, 63.
- <sup>55</sup> [19] <http://wiki.fysik.dtu.dk/dacapo>
- [20] Hammer, B., *et al.*, *Phys. Rev. B*, 1999, **59**, 7413.
- [21] Macounova, K., *et al.*, *J. Solid State Electrochem.*, 2009, **13**, 959.
- [22] Liao, P., *et al.*, *J. Am. Chem. Soc.*, 2012, **134**, 13296.
- <sup>60</sup> [23] Strmcnik, D. *et al.*, *Nat. Chem.*, 2009, **1**, 472.
- [24] Subbaraman, R. *et al.*, *Nat. Mater.*, 2012, **11**, 550.

- [25] Rodriguez, P., Koverga, A. A. & Koper, M. T. M., *Angew. Chem. Int. Ed.*, 2010, **49**, 1241.
- [26] Rodriguez, P., Kwon, Y. & Koper, M. T. M., *Nat. Chem.*, 2012, 177.
- <sup>65</sup> [27] Stamenkovic, V. *et al.*, *Angew. Chem. Int. Ed.*, 2006, **45**, 2897.
- [28] Peterson, A. A. & Norskov, J. K., *J. Phys. Chem. Lett.* 2012, **3**, 251.
- <sup>70</sup> [29] Schouten, K. J. P., *et al.*, *Chem. Sci.*, 2011, **2**, 1902.